

The effect of fluid shear stress on the *in vitro* degradation of poly(lactide-co-glycolide) acid membranes

Zhaowei Chu,^{1*} Quan Zheng,^{1*} Meng Guo,¹ Jie Yao,¹ Peng Xu,¹ Wentao Feng,¹ Yongzhao Hou,¹ Gang Zhou,¹ Lizhen Wang,¹ Xiaoming Li,¹ Yubo Fan^{1,2}

¹Key Laboratory for Biomechanics and Mechanobiology of Ministry of Education, International Research Center for Implantable and Interventional Medical Devices, Key Laboratory for Optimal Design and Evaluation Technology of Implantable & Interventional Medical Devices, School of Biological Science and Medical Engineering, Beihang University, Beijing, People's Republic of China

²National Research Center for Rehabilitation Technical Aids, Beijing, People's Republic of China

Received 7 March 2016; revised 25 April 2016; accepted 26 April 2016

Published online 17 May 2016 in Wiley Online Library (wileyonlinelibrary.com). DOI: 10.1002/jbm.a.35766

Abstract: Poly(lactide-co-glycolide) acid (PLGA) has been widely used as a biodegradable polymer material for coating stents or fabricating biodegradable stents. Its mechanism of degradation has been extensively investigated, especially with regard to how tensile and compressive loadings may affect the *in vitro* degradation of PLGA. Fluid shear stress is also one of the most important factors in the development of atherosclerosis and restenosis. But the effect of fluid shear stress on the degradation process is still unclear. The purpose of this study was to characterize the *in vitro* degradation of PLGA membranes that experienced different fluid shear stresses in 150 mL of deionized water at 37°C for 20 days. Particular emphasis was given to changes in the viscosity of the degradation solution, as well as the mechanical and morphological properties of the samples. The viscosity of the

degradation solution with the mechanical loaded specimens was more severely affected than that of the control group. Increasing the fluid shear stress could accelerate the loss of the ultimate strength of PLGA membranes while it slowed down the change of the tensile elastic modulus in the early period. With regard to morphology, the surface roughness was more obviously reduced in the loaded groups. This indicated that the fluid shear stress could affect the *in vitro* degradation of PLGA membranes. Therefore, this study could help improve the design of PLGA membranes for biomedical applications. © 2016 Wiley Periodicals, Inc. *J Biomed Mater Res Part A*: 104A: 2315–2324, 2016.

Key Words: poly(lactide-co-glycolide) acid, PLGA membranes, fluid shear stress, degradation

How to cite this article: Chu Z, Zheng Q, Guo M, Yao J, Xu P, Feng W, Hou Y, Zhou G, Wang L, Li X, Fan Y. 2016. The effect of fluid shear stress on the *in vitro* degradation of poly(lactide-co-glycolide) acid membranes. *J Biomed Mater Res Part A* 2016;104A:2315–2324.

INTRODUCTION

Since the first use of synthetic biodegradable sutures in the latter half of the 1960s,¹ biodegradable polymers prepared from poly(lactic acid) (PLA), poly(glycolic acid) (PGA), and other degradable poly(α -hydroxy acids) have been widely used in biomedical applications approved by the FDA. Poly(lactide-co-glycolide) acid (PLGA) based on PLA and PGA has been used for fabricating temporary prostheses,^{2–5} three-dimensional porous scaffolds and films,^{6–17} controlled/sustained release drug delivery vehicles,^{18–26} wound closure (surgical sutures and staples),^{27–29} and implantable thera-

peutic devices (orthopedic fixation devices and cardiovascular stents and grafts),^{30–36} all of which have made many significant achievements in tissue engineering, regenerative medicine, gene therapy, controlled drug delivery, and bionanotechnology.³⁷

PLGA has its hydrolytically labile chemical bonds in its backbone and has been shown to primarily undergo bulk degradation *in vivo* via chemical hydrolysis of the hydrolytically unstable ester bonds into lactic acid and glycolic acid. These metabolic products can be excreted from the body by normal metabolic pathways, such as the tricarboxylic acid

*Both authors contributed equally to this study

Correspondence to: Y. Fan; e-mail: yubofan@buaa.edu.cn

Contract grant sponsor: National Natural Science Foundation of China; contract grant numbers: 11120101001, 11421202, 11572029, 31470915, 31370959

Contract grant sponsor: National Science & Technology Pillar Program of China; contract grant numbers: 2014BAI11B02, 2014BAI11B03, 2012BAI18B01

Contract grant sponsor: Beijing Natural Science Foundation; contract grant number: 7142094

Contract grant sponsor: Beijing Science and Technology Plan; contract grant number: Z131100002713018

Contract grant sponsor: Fok Ying Tung Education Foundation; contract grant number: 141039

Contract grant sponsor: Research Fund for the Doctoral Program of Higher Education of China; contract grant number: 20131102130004

cycle. Because of the significantly different biomaterial properties of PLA and PGA, different ratios of PLGAs have been developed to adjust their degradation rate for the intended commercial applications. Particularly, due to the great biocompatibility and good processability of PLGA, it has promising applications in the field of percutaneous angioplasty and stenting treatment, as PLGA can be utilized for coating drug-eluting stents (DES) and fabricating biodegradable polymers is that of heart patches, as they can be used to regenerate heart tissue.³⁸

During the implantation, biodegradable medical devices composed of PLGA-like vascular stents and heart patches are supposed to have the mechanical properties (such as strength and stiffness) of the surrounding tissue and the adequate degradation time, which matches the healing process or regeneration rate of the tissue. But the physiological and biochemical environments *in vivo* are too complex to keep the degradation rate of PLGA at ideal rate. So, extensive investigations have been performed to evaluate the effect of each of these variables on degradation. Accordingly, the rate of PLGA degradation depends not only on its inherent properties, including the PLA/PGA ratio, molecular weight and distribution, shape, morphology, and level of crystallinity^{39–44} but also on other chemical and biochemical environmental factors, such as the degradation medium, pH value, temperature, and enzymatic activity.^{45–47} In addition, various local and gross mechanical loads from different tissues during maintenance may influence the rate of degradation. In turn, the structural, morphological and mechanical properties of PLGA may also be affected during degradation. As such, the relationship between the mechanical load environment and the degradation of PLGA has also been investigated.^{48–52} Generally, tensile, compressive, and shear loads are the main types of mechanical loadings that occur *in vivo*. Our previous study reported that tensile load, compressive load, and the combination of tensile plus compressive loads accelerated the *in vitro* degradation of poly (D,L-lactic acid) compared to those without such mechanical loads.⁵³ Subsequent studies demonstrated that the tensile load increased the degradation rate of electrospun PLGA *in vitro*,⁵⁴ but the effect of cyclic loading on *in vitro* degradation of porous PLGA scaffolds was more complex.⁵⁵ Guo M et al.⁵⁶ developed a model to describe the relationship between the tensile stress and degradation rate of PLGA. Fluid shear stress is the most common type of mechanical loading generated by blood flowing in human vessels and plays an important role in the development of atherosclerosis and restenosis.⁵⁷ Autopsy studies showed that even 40 months beyond implantation, the stents were not fully endothelialized,⁵⁸ and the coating polymer material was exposed to flowing blood. It is reasonable to assume that the fluid shear stress has the effect on the degradation process of biodegradable material, such as PLGA; however, it is still not well understood.

The purpose of this research was to characterize the effect of fluid shear stress on the hydrolytic degradation of PLGA membranes. Custom designed devices were used to

apply fluid shear stresses onto PLGA membranes over a pre-designated time. *In vitro* degradation behaviors of PLGA membranes without and with different fluid shear stresses in deionized water at a constant temperature were compared in detail, with emphasis on changes in the viscosity of the degradation solution and alterations in the mechanical and morphological properties of the samples. This research could help improve the design of PLGA membranes matching the healing or generation process for biomedical applications.

MATERIALS AND METHODS

Materials

PLGA powder (copolymerization ratio of PLA/PGA = 50/50) was purchased from DaiGang Co. (Shandong, People's Republic of China). The average molecular weight was about 10×10^4 Da, and the polydispersity index was about 1.5. Chloroform and 1,4-dioxane were analytical grade and obtained from Aoli Co. (Beijing, People's Republic of China).

Fabrication of PLGA membranes

PLGA membranes were prepared by the solvent-casting method. A total of 100 mg of PLGA powder were individually placed into 10 mL of organic solvent composed of chloroform and 1,4-dioxane to produce a polymer of 1% (w/v) in concentration. 1,4-Dioxane, which volatilized slower, was added to the chloroform with a volume ratio of 5:13 to provide a proper velocity of volatilization for the preparation of uniform membranes. After complete dissolution, the solution was poured onto a customized glass sheet (150 mm \times 50 mm) fixed on a horizontal table. The thicknesses of samples were detected by the micrometer, and the average thickness is $0.11 \text{ mm} \pm 0.01 \text{ mm}$. The samples were dried for 4 days at room temperature (25°C) in air and then put in a vacuum drying oven for another 7 days also at room temperature (25°C) to remove any remaining organic solvent. Residual chloroform and 1,4-dioxane in the films were not detected using gas chromatography (Agilent, Palo Alto, CA) with the carrier gas of nitrogen.

The circulating system

The circulating system is shown in Figure 1. The system was composed of the following parts: a peristaltic pump, a receiver, two capacitors and two resistors, a self-designed flow chamber, and connecting tubes. The degradation solution was driven by a peristaltic pump (Masterflex L/S; Cole-Parmer), which is the power, and smoothed by liquid capacities and liquid resistances. The flow chamber made of polycarbonate plastic was custom-developed in this study. The whole structure could be autoclaved. The flow chamber consisted of two plates sealed by an O-ring. The upper plate was equipped with two reservoirs and two branch tubes as the flow inlet and outlet separately. The bottom plate had a groove for fixing the PLGA membranes with glass sheets. The height of the flow chamber was determined by the thickness of the silicon gasket, 0.3 mm in this study. There was an effective region defined between the two reservoirs on the membranes.

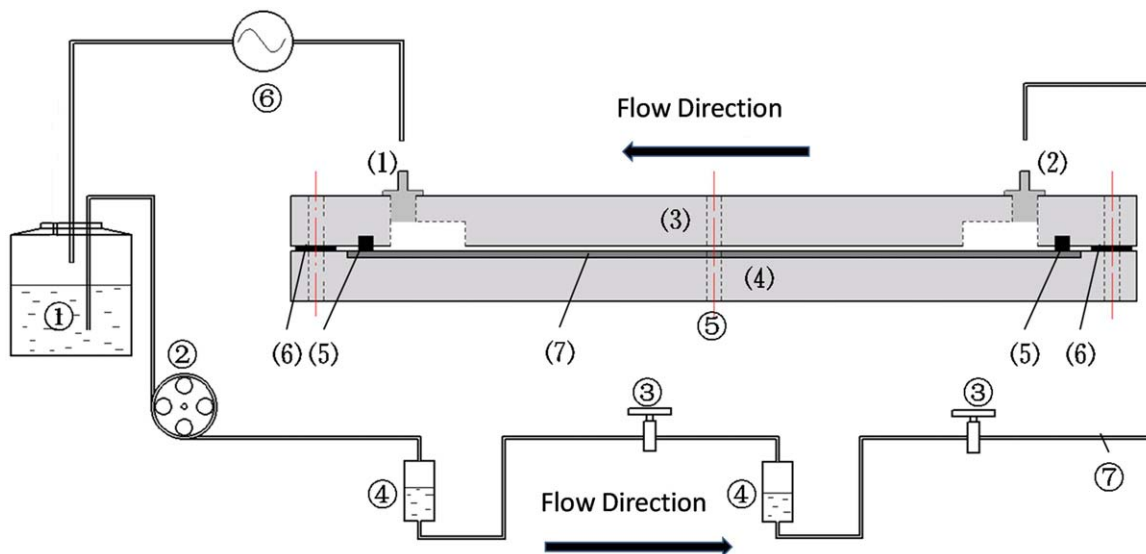


FIGURE 1. Schematic diagram of the circulating system and details of the parallel plate flow chamber: ① receiver, ② peristaltic pump, ③ liquid resistance, ④ liquid capacity, ⑤ self-designed flow chamber, ⑥ flow meter, and ⑦ connecting tubes: (1) outlet joint, (2) inlet joint, (3) top PC plate, (4) bottom PC plate, (5) O-ring, (6) silicone gasket, and (7) glass sheet with PLGA membrane.

Validation of the flow chamber was carried out using a finite volume technique-based commercial package (FLUENT 6.3.26; ANSYS, Canonsburg, PA). The computational grid domain of the flow chamber is depicted in Figure 2, including the inlet tube, outlet tube, two reservoirs, and the effective region.

***In vitro* degradation studies**

The *in vitro* degradation studies of the PLGA membranes were conducted in 150 mL sterilized deionized water with an original pH value of 7.4 and maintaining the intensity of

the fluid shear stress applied within the physiological range, 10–40 dyn/cm² in large arteries.⁵⁹ Since dry PLGA membranes bloat due to water absorption upon immersion in deionized water, all the specimens with glass sheets were prepared in advance in deionized water for 1 hour, and then the glass sheets with PLGA membranes were fixed into the device. For comparison, the control PLGA degradation experiments without fluid shear stress were conducted in plastic vessels containing 150 mL of deionized water. Three experiments for different shear stresses were conducted. In groups 1–3, the flow rates were set to be 10, 16.7, and

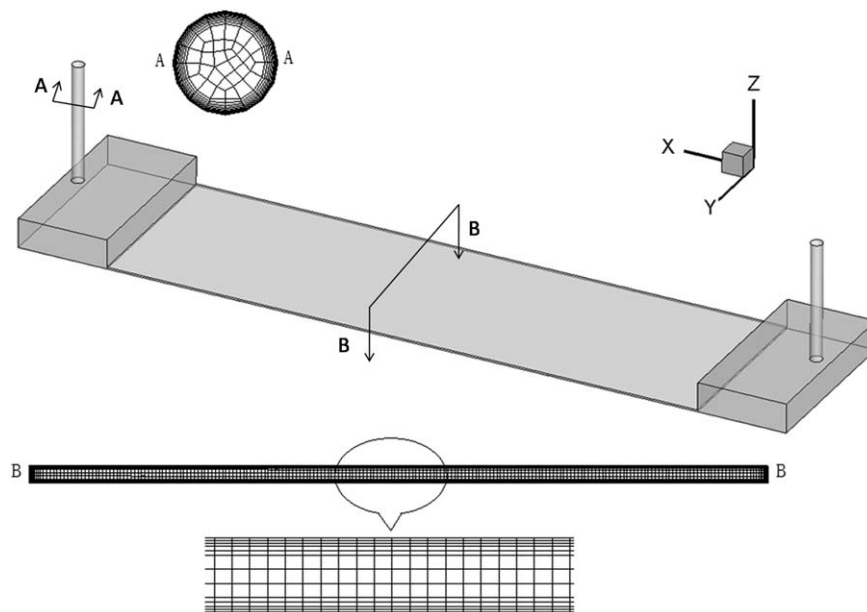


FIGURE 2. The computational grid domain of the flow chamber.

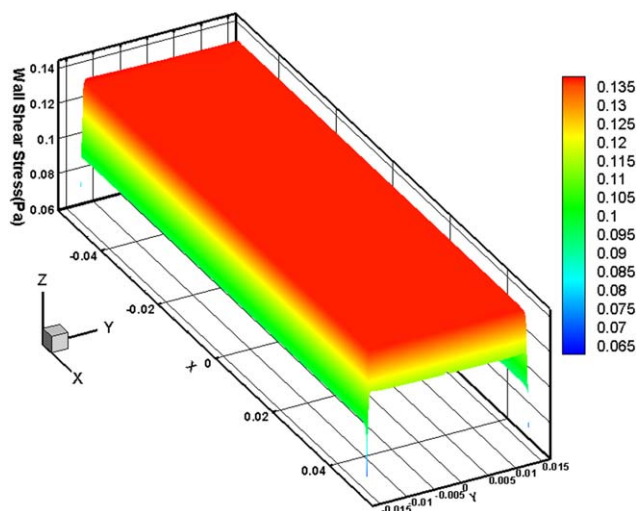


FIGURE 3. Contour plot of wall shear stress distribution in the membrane's effective region.

25 mL/min, separately, which maintained the fluid shear stress at 12, 20, and 30 dyn/cm².

All the degradation experiments were carried out at a constant temperature of 37°C in a water bath. Every 5 days, the degradation solution was collected for viscosimetric tests, and six specimens in each group were taken out for mechanical tests and surface morphology observation. All the samples were washed with distilled water three times, removed from the glass sheet, and then dried at room temperature for at least 48 hours.

Viscosimetric test

The viscosities of the degradation solution were determined periodically by using a cone-and-plate viscometer (R/S plus RHEOMETER; BROOKFIELD). At each test point, six groups of 3.9 mL degradation solution were taken out. Every measurement was carried out at a rotation of 240 rpm for 2 minutes at room temperature (25°C). Twenty-one values were taken for each 2 minutes.

Mechanical properties

After been got rid of the nonuniform shear stress region, each large specimen was cut into six strips (50 mm × 10 mm) for mechanical testing. The tensile elastic modulus E , ultimate strengths σ , and break elongation ϵ_t of six specimens before and after *in vitro* degradation were measured using a materials testing machine (ElectroPuls™ E10000; INSTRON). A 250N tension sensor was used, and tests were run at 1 mm/min. All tests were conducted at room temperature.

Morphologies

Scanning electron microscopy (SEM) (SNE-3200M; SEC, Korea) was used to observe the surface morphology of the PLGA specimens at 300× magnification as they degraded over time. SEM observation was carried out at 30 kV. Dried specimens were prepared and sputter-coated with a gold layer before observation.

RESULTS

Validation of the flow chamber

Figure 3 reveals the simulated distribution of the wall shear stress at the membrane's effective region. The area ratio of the uniform wall shear stress region to the whole effective region was >95%. The left nonuniform region could be noticed of a distribution near the wall due to the boundary layer effect. This result suggested that the custom flow chamber could reliably apply a steady fluid shear stress on membranes.

Viscosimetric test

The changes in viscosities of the degradation solution in each group before and after different days of degradation *in vitro* are shown in Figure 4. After the first 5 days of degradation, a sharp increase in viscosity was observed in all groups. In particular, the viscosity of the degradation solution in the third group with a fluid shear stress of 30 dyn/cm² increased to 1.87 ± 0.06 mPa s, marking a rise of about 44% when compared to the original level of deionized water, 1.30 mPa s, but the control group and group 1 only saw an increase of 25% and 28%, respectively. After 10 days of degradation, the viscosities dropped to an average level of about 1.53 mPa s, which was still greater than the viscosity of deionized water. From day 10 onward, the viscosities increased gradually by 37%, 38%, 44%, and 28% during the last 10 days of degradation, reaching a final value of 1.78 ± 0.05, 1.80 ± 0.03, 1.87 ± 0.04, and 1.66 ± 0.07 mPa s in each group, respectively.

Changes in mechanical properties

The mechanical properties of PLGA membranes are illustrated in Figure 5(a-c), which reveals the changes in terms of tensile elastic modulus E , break elongation ϵ_b , and ultimate strength σ with advances in the degradation process under different fluid shear stresses.

As shown in Figure 5(a), the tensile elastic modulus of the unloaded PLGA membranes remained nearly constant

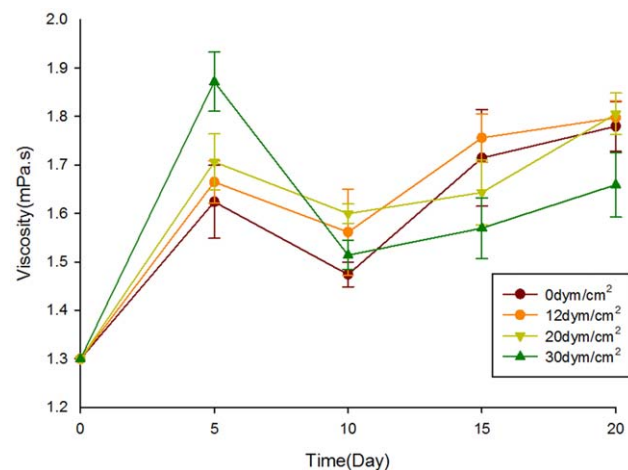


FIGURE 4. Changes in viscosities of the degradation solution with different fluid shear stresses as a function of the degradation time. The results are presented as mean ± standard deviation ($n = 20$).

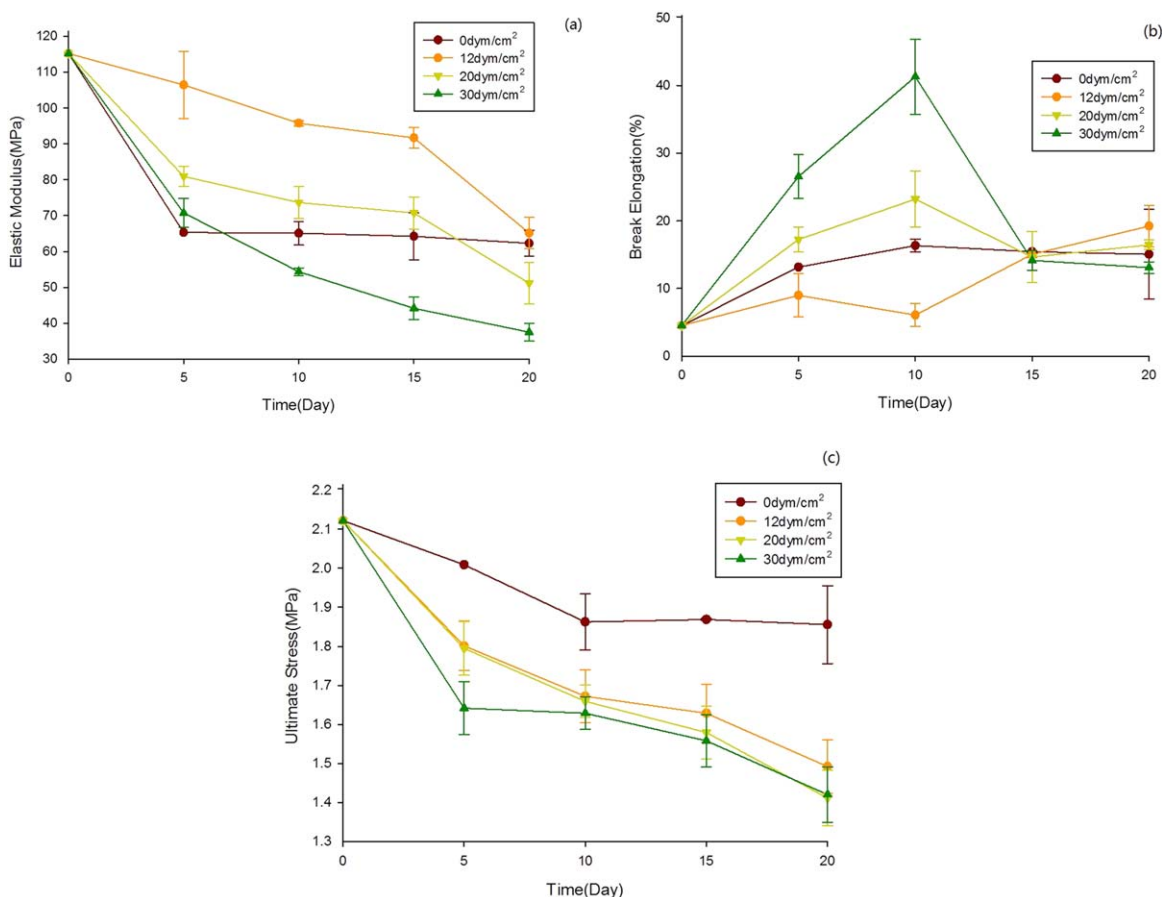


FIGURE 5. Changes in terms of (a) tensile elastic modulus E , (b) break elongation ϵ_b , and (c) ultimate strengths σ as a function of the degradation time with different fluid shear stresses. The results are presented as mean \pm standard deviation ($n = 6$).

after 5 days of degradation, while that of fluid shear stress loaded membranes changed dramatically during 15 days of degradation. In the control group, the tensile elastic modulus decreased sharply to 65.29 ± 3.26 MPa at the end of the fifth day (56.7% of the original value) and then dropped a further 3.01 MPa to reach 62.28 ± 7.63 MPa after another 15 days. The tensile elastic modulus of the loaded PLGA membranes decreased more apparently after the total allowable degradation period had passed, resulting to a final value of 65.13 ± 4.37 , 51.14 ± 5.82 , and 37.49 ± 2.50 MPa in groups 1–3 (about 56.53%, 44.39%, and 32.54% of the original value).

The changes in break elongation can be seen in Figure 5(b). The profiles behaved nearly the opposite to the tensile elastic modulus. In the control group, the break elongation of PLGA membranes increased during the first 10 days of degradation and then remained almost constant to the end. The magnitude rose from the original 4.52% to $15.07 (\pm 0.07)\%$, resulting in a growth of 333.66%. The change in break elongation in group 1 was not as dramatic during the first 10 days, but only approximately doubled the original level. However, the trend did not stagnate after the 10th day as in the control group, but the value kept rising, reaching $19.23 (\pm 0.03)\%$ at day 20. Groups 2 and 3 showed more dramatic changes during the first 10 days, reaching a maximum value of

$23.21 (\pm 0.04)\%$ and $41.29 (\pm 0.06)\%$ separately (almost five and ten times the original value). Then, it began to fall sharply below the level of the control group before plateauing on 15th day until the end.

Figure 5(c) reveals the changes in the ultimate strength of PLGA membrane as a function of the degradation time. Similar to the tensile elastic modulus, the ultimate strength of the PLGA membranes in the control group decreased continuously, reaching almost 12% of their initial value (2.12 MPa) at the end of day 10, while by day 20, it had dropped to 1.86 ± 0.13 MPa. The plots for the other groups were close and followed a similar trend. In groups 1 and 2, after a sharp decrease during the first 10 days, the ultimate strength reached 1.67 ± 0.07 and 1.66 ± 0.04 MPa, then dropped slightly further during days 10–15, followed by a more rapid decrease to 1.49 ± 0.07 and 1.41 ± 0.07 MPa by day 20. Following the same tendency, the specimens from group 3 lost 22% of their ultimate strength in the first 5 days of degradation. However, the ultimate strength reached a final magnitude of 1.42 ± 0.07 MPa close to group 2 by the end of the test period.

Morphologies

Figure 6 presents SEM micrographs of the surface morphology of the PLGA membranes in terms of degradation time

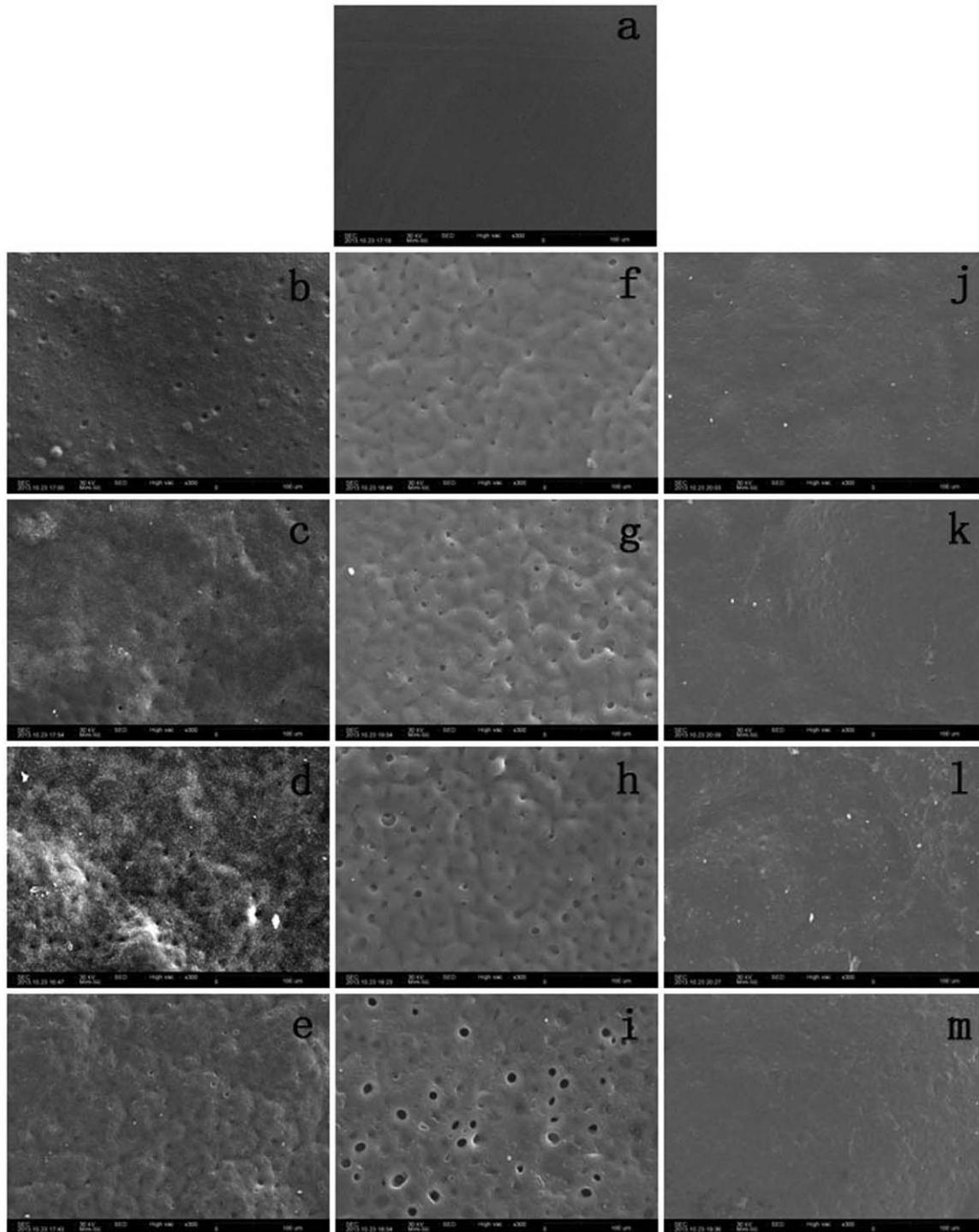


FIGURE 6. PLGA morphology before and after degradation with different fluid shear stresses. (a) Before degradation; unloaded degradation after (b) 5 days, (c) 10 days, (d) 15 days, and (e) 20 days; at a fluid shear stress of 12 dyn/cm² after (f) 5 days, (g) 10 days, (h) 15 days, and (i) 20 days; and at a fluid shear stress of 30 dyn/cm² after (j) 5 days, (k) 10 days, (l) 15 days, and (m) 20 days.

and under different applied fluid shear stresses. As can be seen in Figure 6(a), the surface of the PLGA membranes without being immersed or loaded was flat, smooth, and without pores. After immersion in the degradation solution, all membrane surfaces became quite opaque and whitened. Within 5 days, small irregular pores appeared on the sur-

face [Figure 6(b)], and then the membranes roughened due to water absorption [Figure 6(c)]. As the degradation time increased, the pore size and depth also increased, along with the distribution density of the pores [Figure 6(d)]. Finally, specimens in the control group had a rough surface of randomly distributed pores. Membranes from group 1

displayed a different degradation pattern. At the beginning of the experiment, the pores were distributed more uniformly and densely but not as deep as in the control group [Figure 6(f)]. Then, the micropores expanded in size and depth, but the quantity remained somewhat unchanged [Figure 6(g,h)]. The pores expanded a great deal and even penetrated through the membranes during the last 5 days of degradation [Figure 6(i)]. In contrast, although the PLGA membranes in group 3 lost their transparency, the surfaces were noticeably flatter and smoother. Few surface pores appeared from the beginning of the degradation test to the end. These pores changed slightly during the whole period and did not influence the macroscopical morphology of the surface.

DISCUSSION

A number of devices have been investigated for providing suitable mechanical stimuli to simulate the environment *in vivo*. The custom flow chamber used in this research was designed to apply a steady fluid shear stress to membranes *in vitro*. Since it was difficult to validate the fluid wall shear stress generated with existing test methods, a computational simulation was conducted. The solution flowed through the interior domain of the flow chamber, generating fluid wall shear stress on the surface of membranes. The shear stress magnitude could be adjusted by changing the flow rate of the solution.

The viscosity of the degradation solution is one of the properties used to characterize lactic acid release and is correlated with the molecular weight that remained in solution over the whole *in vitro* degradation process. It was clearly observed that the changes in viscosity of the PLGA membrane degradation solution were dramatic during the degradation period but followed the same tendency after being exposed to deionized water at 37°C. The changes that occurred during the first 5 days for all conditions were mainly associated with the release of unbonded large molecular weight fragments from the surface of PLGA into the solution. Moreover, a positive correlation between the magnitude of the fluid shear stress and the increase in viscosity was found during this period. It is commonly recognized that once the larger molecular fragments diffuse or wash out, they will be in contact with a large excess of solution and reasonably degrade into low molecular weight fragments, or even into monomeric units of lactic and glycolic acids. Therefore, at the end of day 10, a sharp decrease in viscosity occurred. From day 10 onward, the viscosities increased with different extend in all groups. It has been suggested that as the hydration process continues, the porous membrane surface allows more water molecules to enter into the interior of the PLGA and more fragments caused by massive cleavage of the backbone covalent bonds diffuse into the solution, which promotes the initial degradation.

The tensile elastic modulus, ultimate strengths, and break elongation are the typical parameters of interest when tensile testing the PLGA membrane specimens after undergoing different degradation periods. However, only the

strain, tensile, and compressive load rather than the fluid shear stress load had been performed to examine the mechanical properties of PLGA as it degrades.⁴⁸⁻⁵⁶ As reported by Vey et al.,⁶⁰ as soon as the membranes were immersed in the solution, the water molecules diffused into the interior matrix of the polymer, which caused a soft surface layer to form while the bottom layer remained relatively hard. From a microscopic point of view, because of the existence of the flow flux, the circulating system kept the water molecules running, the water molecules could difficultly diffuse further into the membranes, resulting in a much thinner soft layer in fluid shear stress loaded groups. That might be the reason why in the control group more decrease of tensile elastic modulus were observed, which is a parameter that measures the membranes' resistance to being deformed elastically when subjected to forces. Meanwhile, the fluid shear stress stretched the soft surface of the specimens, and the flow caused more fresh water molecules diffuse into the interior matrix to conduct backbone chain scission, making the soft layer much more friable. This could explain the observed more decrease in ultimate strength in the fluid shear stress loaded groups after the first 5 days. Due to the water absorption, water molecules diffused into the interior matrix of the polymer and helped accelerate the relaxation of membranes, leading to a larger matrix volume. After being dried in room temperature, the specimens shrunk much more due to the larger matrix volume, resulting in an increase in the break elongation in all groups at day 5. Besides, it showed that there was a positive correlation between the changes in tensile elastic modulus, break elongation and ultimate strength and the magnitude of fluid shear stress over this first period. However, the break elongation is related to the degree of shrink and the ability to stretch of the harder layer. So the break elongation showed less increase when compared to the control group. Thereafter, almost from day 10, all the samples in the control group absorbed enough water to be all softened, resulting in slow bulk degradation. As the hydrolysis created more acids in the water-filled pores, the autocatalytic phenomenon processed.⁶¹ So, all parameters of interest showed little decrease in the control group. This result is consistent with data reported by Li P et al.⁵⁴ However, dramatic changes were observed in other groups. With increasing degradation time, the soft layer kept growing further and further into the bottom layer, leading to the continuous decrease of the tensile elastic modulus. Besides, all the structure became weaker and weaker because of the chain scission and further degradation, leading to continuous decrease of ultimate strength, which is the capacity of the membranes to withstand loads tending to elongate. It is worth noting that during the 10-15 days degradation, all the samples in all groups were softened, and the break elongation converged at day 15. Because of the mass transport of flow, more fresh water molecular could diffuse into the pores, and degradation products could be washed out. So, the tensile elastic modulus and ultimate strength were dramatically altered in loaded groups due to fluid-induced degradation along with degradation. From the above, fluid

shear stress can be implicated in accelerating the loss of the ultimate strength of PLGA membranes while slowing down the change of the tensile elastic modulus in the early period.

Micrographs of the surface taken at different degradation times were also revealed (Figure 6). After immersion, all specimens became cloudy and noticeably whiter. The loss of transparency could be attributed not only to water absorption, but also to the development of pores, voids, inclusions or spherulites.¹⁹ Water absorption also corresponded to a huge decrease in molecular weight due to chain scission of polyester bonds during hydrolysis.^{62,63} As reported by Vey et al.,⁶⁰ a top soft surface layer formed when PLGA membranes were immersed in the degradation solution during the early stages of degradation, small pores, or holes appeared on the amorphous surface region of the PLGA membranes in the control group [Figure 6(b)]. The degradation products released in these pores obstructed from diffusing out and would play a negative part to accelerate the degradation process. Subsequently, the number and depth of pores increased gradually, following the appearance of wrinkles on the surface [Figure 6(d)]. A rough surface developed finally while the remaining backbone did not change much. So, there were only minor changes in the parameters of interest. In contrast, in group 1, micropores formed more uniformly in the early stage membrane surfaces [Figure 6(f)]. With increasing degradation time, the soft surface layer thickened, the quantity of macropores increased, and the number of micropores remained relatively constant. In this period, the hard bottom layer prevented the tensile elastic modulus and break elongation from changing rapidly until after 15 days of degradation. Since the fluid could flush the degradation products out of the micropores and make more water available for molecular cleavage of covalent bonds in the PLGA polymer backbone, the pores were getting larger and even penetrated at the whole sample [Figure 6(i)]. Furthermore, due to the stretching effect of fluid shear stress, the roughness of the surface reduced. In group 3, the fluid shear stress rather than the mass transport played an important role in smoothing the soft surface layer, resulting in a flatter surface [Figure 6(m)]. This could also be related with the uniform surface hydrolysis as the consequence of minimum localized autocatalyzed hydrolysis. It is reasonable to assume that the fluid shear stress has a great effect on surface morphology.

Understanding the influence in fluid shear stress on the degradation of PLGA is helpful for effective prediction of the *in vivo* degradation dynamics, which is important in developing appropriate biodegradable medical implants and drug delivery system made of PLGA. This work may improve a better design for the coating of DES and biodegradable stents that may not fully endothelialized⁵⁸ and only covered by scattered thrombus or fibrin, but there are limitations in the study. First, it ignores the change of the fluid shear stress magnitude with macro changes in surface morphology during the degradation period. Second, 150 mL of sterilized deionized water was used as degradation solution, which was much more than usual. However, the local pH changes are ignored during the period. Third, according to

our results, the changes in viscosities of the degradation solution had been observed during the degradation process in all groups. So, it is reasonable to assume that the viscosity as other factors, such as pH, has effect on the degradation process, but why and how the viscosity affects are still not clear. These will be in our future work. Fourth, as concluded, increasing the fluid shear stress could accelerate the loss of the ultimate strength of PLGA membranes while slowing down the change of the tensile elastic modulus in the early period. More future evidence including SEM at cross section and material crystalline should be done on the mechanism or degradation pattern. Fifth, the experimental conditions are different from the true *in vivo* degradation environment; more factors, such as pH, and temperature should be considered.

CONCLUSIONS

The fluid shear stress affects the viscosity of the degradation solution and accelerates the loss of the ultimate strength of PLGA membranes while it slows down the change of the tensile elastic modulus in the early period. The fluid shear stress has a great effect on the surface morphology of PLGA membranes. This study is helpful for understanding the influence of fluid shear stress on the *in vitro* degradation process of PLGA membranes. The degradation of PLGA under physiological pulsatile flow and the effect of mass transport on the *in vitro* degradation process should be further investigated. It is deduced that the *in vivo* degradation of PLGA implants under fluid shear stress should be carefully considered to advance appropriate degradation design for matching the healing or generation process in the biodegradable medical applications.

ACKNOWLEDGMENT

We thank Dr. Ping Li for her very kind suggestions on the study design and results analysis.

REFERENCES

1. Barbucci R. Integrated Biomaterial Science. New York: Kluwer Academic/Plenum Publishers; 2002.
2. Angelova N, Hunkeler D. Rationalizing the design of polymeric biomaterials. Trends Biotechnol 1999;17:409–421.
3. Dee KC, Puleo DA, Bizios R, editors. An Introduction to Tissue–Biomaterial Interactions. New York: John Wiley and Sons; 2002.
4. Ratner BD, Hoffman AS, Schoen FJ, Lemons JE, editors. Biomaterials Science: An Introduction to Materials in Medicine. Amsterdam: Elsevier Academic Press; 2004.
5. Neut D, Dijkstra RJ, Thompson JI, Kavanagh C, van der Mei HC, Busscher HJ. A biodegradable gentamicin-hydroxyapatite-coating for infection prophylaxis in cementless hip prostheses. Eur Cells Mater 2015;29:42–56.
6. Freed LE, Gordana VN, Langer R. Biodegradable polymer scaffolds for tissue engineering. Biotechnology 1994;12:689–693.
7. Chu CC. Biodegradation properties. In: Chu CC, von Fraunhofer JA, Greisler HP, editors. Wound Closure Biomaterials and Devices. Boca Raton, FL: CRC Press; 1997. p 182–183.
8. Peter SJ, Miller MJ, Yasko AW, Yaszemski MJ, Mikos AG. Polymer concepts in tissue engineering. J Biomed Mater Res 1998;43: 422–427.
9. Holy CE, Shoichet MS, Davies JE. Engineering three-dimensional bone tissue *in vitro* using biodegradable scaffolds: Investigating initial cell-seeding density and culture period. J Biomed Mater Res 2000;51:376–382.

10. Riddle KW, Mooney DJ. Role of poly(lactide-co-glycolide) particle size on gas-foamed scaffolds. *J Biomater Sci Polym Ed* 2004;15:1561–1570.
11. Yue H, Zhang L, Wang Y, Liang F, Guan L, Li S, Yan F, Nan X, Bai C, Lin F, Yan Y, Pei X. Proliferation and differentiation into endothelial cells of human bone marrow mesenchymal stem cells (MSCs) on poly-dl-lactic-co-glycolic acid (PLGA) films. *Chinese Sci Bull* 2006;51:1328–1333.
12. Yang Y, Zhao Y, Tang G, Li H, Yuan X, Fan Y. In vitro degradation of porous poly(L-lactide-co-glycolide)/ β -tricalcium phosphate (PLGA/ β -TCP) scaffolds under dynamic and static conditions. *Polym Degrad Stab* 2008;93:1838–1845.
13. Yu D, Li Q, Mu X, Chang T, Xiong Z. Bone regeneration of critical calvarial defect in goat model by PLGA/TCP/rhBMP-2 scaffolds prepared by low-temperature rapid-prototyping technology. *Int J Oral Max Surg* 2008;37:929–934.
14. Hu X, Shen H, Yang F, Bei J, Wang S. Preparation and cell affinity of microtubular orientation-structured PLGA (70/30) blood vessel scaffold. *Biomaterials* 2008;29:3128–3136.
15. He Zeqiang, Xiong L. A comparative study on in vitro degradation behaviors of poly(L-lactide-co-glycolide) scaffolds and films. *J Macromol Sci Part B* 2010;49:66–74.
16. Li XM, Yang Y, Fan YB, Feng QL, Cui FZ, Watari F. Biocomposites reinforced by fibers or tubes, as scaffolds for tissue engineering or regenerative medicine. *J Biomed Mater Res Part A* 2014;102:1580–1594.
17. Li XM, Wang Z, Zhao TX, Yu B, Fan YB, Feng QL, Cui FZ, Watari F. A novel method to in vitro evaluate biocompatibility of nano-scaled scaffolds for tissue engineering with neutrophils. *J Biomed Mater Res Part A* 2016. doi:10.1002/jbm.a.35743.
18. Cohen S, Yoshioka T, Lucarelli M, Hwang LH, Langer R. Controlled delivery systems for proteins based on poly(lactic/glycolic acid) microspheres. *Pharm Res* 1991;8:713–720.
19. Park TG, Lu WQ, Crotts G. Importance of in vitro experimental conditions on protein release kinetics, stability and polymer degradation in protein encapsulated poly(d,l-lactic-co-glycolic acid) microspheres. *J Control Release* 1995;33:211–22.
20. Jain RA. The manufacturing techniques of various drug loaded biodegradable poly(lactide-co-glycolide) (PLGA) devices. *Biomaterials* 2000;21:2475–2490.
21. Friess W, Schlapp M. Release mechanisms from gentamicin loaded poly(lactic-co-glycolic acid) (PLGA) microparticles. *J Pharm Sci* 2002;91:845–855.
22. Schwendeman SP. Recent advances in the stabilization of proteins encapsulated in injectable PLGA delivery systems. *Crit Rev Ther Drug Carrier Syst* 2002;19:73–98.
23. Taluja A, Yu SY, You HB. Novel approaches in microparticulate PLGA delivery systems encapsulating proteins. *J Mater Chem* 2007;17:4002–4014.
24. Semete B, Booyesen L, Lemmer Y. In vivo evaluation of the biodistribution and safety of PLGA nanoparticles as drug delivery systems. *Nanomed Nanotechnol Biol Med* 2010;6:662–671.
25. Li XM, Zhao TX, Sun LW, Aifantis KE, Fan YB, Feng QL, Cui FZ, Watari F. The applications of conductive nanomaterials in the biomedical field. *J Biomed Mater Res Part A* 2016;104:320–337.
26. Li XM, Wei JR, Aifantis KE, Fan YB, Feng QL, Cui FZ, Watari F. Current investigations into magnetic nanoparticles for biomedical applications. *J Biomed Mater Res Part A* 2016;104:1285–1296.
27. Benicewicz BC, Hopper PK. Polymers for absorbable surgical sutures. *J Bioact Compat Polym* 1991;6:64–94.
28. Zacchi V, Soranzo C, Cortivo R, Radice M, Brun P, Abatangelo G. In vitro engineering of human skin-like tissue. *J Biomed Mater Res* 1997;36:17–28.
29. Khorsand-Ghayeni M, Sadeghi A, Nokhasteh S, Molavi AM. Collagen modified PLGA nanofibers as wound-dressing. In: *The International Conference on Nanostructures*; 2016.
30. Gibbons DF. Tissue response to resorbable synthetic polymers. In: Plank H, Dauner M, Renardy M, editors. *Degradation Phenomena on Polymeric Biomaterials*. New York: Springer; 1992. p 97–104.
31. Kleinschmidt JC, Marden LJ, Kent D, Quigley N, Hollinger JO. A multiphase system bone implant for regenerating the calvaria. *Plast Reconstr Surg* 1993;91:581–588.
32. Ishaug-Riley SL, Crane GM, Gurlek A, Miller MJ, Yasko AW, Yaszemski MJ, Mikos AG. Ectopic bone formation by marrow stromal osteoblast transplantation using poly(dl-lactic-co-glycolic acid) foams implanted into the rat mesentery. *J Biomed Mater Res* 1997;36:1–8.
33. Westedt U, Wittmar M, Hellwig M, et al. Paclitaxel releasing films consisting of poly(vinyl alcohol)-graft-poly(lactide-co-glycolide) and their potential as biodegradable stent coatings. *J Control Release* 2006;111:235–246.
34. Xintong W, Venkatraman SS, Boey FYC, et al. Controlled release of sirolimus from a multilayered PLGA stent matrix. *Biomaterials* 2006;27:5588–5595.
35. Xiaoxiang Z, Braatz RD. Modeling and analysis of drug-eluting stents with biodegradable PLGA coating: Consequences on intravascular drug delivery. *J Biomech Eng* 2014;136:11.
36. Zhu X, Braatz RD. A mechanistic model for drug release in PLGA biodegradable stent coatings coupled with polymer degradation and erosion. *J Biomed Mater Res Part A* 2014;103:2269–2279.
37. Shalaby SW, Burg KJL. *Absorbable and Biodegradable Polymers (Advances in Polymeric Materials)*. BocaRaton: CRC Press, 2003.
38. Tallawi M, Zebrowski DC, Rai R, Roether JA, Schubert DW, El Fray M, Engel FB, Aifantis KE, Boccaccini AR. Poly(glycerol sebacate)/poly(butylene succinate-dilinoate) (PGS/PBS-DLA) fibrous scaffolds for cardiac tissue engineering. *Tissue Eng C* 2015;21:585–596.
39. Athanasiou KA, Schmitz JP, Agrawal CM. The effect of porosity on *in vitro* degradation of polylactic acid–polyglycolic acid implants used in repair of particular cartilage. *Tissue Eng* 1998;4:53–63.
40. Hurrell S, Cameron RE. The effect of initial polymer morphology on the degradation and drug release from polyglycolide. *Biomaterials* 2002;23:2401–2409.
41. Park TG. Degradation of poly(d,l-lactic acid) microspheres: Effect of molecular weight. *J Control Release* 1994;30:161–173.
42. Park TG. Degradation of poly(lactic-co-glycolic acid) microspheres: Effect of copolymer composition. *Biomaterials* 1995;16:1123–1130.
43. Victor JC, Peter XM. The effect of surface area on the degradation rate of nanofibrous poly(l-lactic acid) foams. *Biomaterials* 2006;27:3708–3715.
44. Wu XS, Wang N. Synthesis, characterization, biodegradation, and drug delivery application of biodegradable lactic/glycolic acid polymers. Part II: Biodegradation. *J Biomater Sci Polym Ed* 2001;12:21–34.
45. Agrawal CM, Huang D, Schmitz JP, Athanasiou KA. Elevated temperature degradation of a 50:50 copolymer of PLA–PGA. *Tissue Eng* 1997;3:345–352.
46. Banu ZS, Burgess DJ. Effect of acidic pH on PLGA microsphere degradation and release. *J Control Release* 2007;122:338–344.
47. Li SM, Girard A, Garreau H, Vert M. Enzymatic degradation of polylactide stereocopolymers with predominant d-lactyl contents. *Polym Degrad Stab* 2001;71:61–67.
48. Miller ND, Williams DF. The *in vivo* and *in vitro* degradation of poly(glycolic acid) suture material as a function of applied strain. *Biomaterials* 1984;5:365–368.
49. Chu CC. Strain-accelerated hydrolytic degradation of synthetic absorbable sutures. In: Hall CW, editor. *Surgery Research—Recent Development*. New York: Pergamon Press; 1985. p 111–115.
50. Zhong SP, Doherty PJ, Williams DF. The effects of applied strain on the degradation of absorbable suture *in vitro*. *Clin Mater* 1993;14:183–189.
51. Deng M, Zhou J, Chen G, Burkley D, Xu Y, Jamiolkowski D, Barbolt T. Effect of load and temperature on *in vitro* degradation of poly(glycolide-co-l-lactide) multifilament braids. *Biomaterials* 2005;26:4327–4336.
52. Deng M, Chen G, Burkley D, Zhou J, Jamiolkowski D, Xu Y, Vetrelin R. A study on *in vitro* degradation behavior of a poly(glycolide-co-l-lactide) monofilament. *Acta Biomater* 2008;4:1382–1391.
53. Fan YB, Li P, Zeng L, Huang XJ. Effects of mechanical load on the degradation of poly(d,l-lactic acid) foam. *Polym Degrad Stab* 2008;9:677–683.
54. Li P, Feng XL, Jia XL, Fan YB. Influences of tensile load on *in vitro* degradation of an electrospun poly(lactide-co-glycolide) scaffold. *Acta Biomater* 2010;6:2991–2996.
55. Yang YF, Tang GW, Zhao YH, Yuan XY, Fan YB. Effect of cyclic loading on *in vitro* degradation of poly(l-lactide-co-glycolide) scaffolds. *J Biomater Sci Polym Ed* 2010;21:53–66.

56. Guo M, Chu ZW, Yao J, Feng WT, Wang YX, Wang LZ, Fan YB. The effects of tensile stress on degradation of biodegradable PLGA membranes: A quantitative study. *Polym Degrad Stab* 2015. doi:10.1016/j.polymdegradstab.2015.12.019.
57. Wentzel JJ, Krams R, Schuurbiens CH, Slager CJ. Relationship between neointimal thickness and shear stress after Wallstent implantation in human coronary arteries. *Circulation* 2001;103:1740–1745.
58. Joner M, Finn AV, Farb A, Mont EK, Kolodgie FD, Ladich E, Kutys R, Skorija K, Gold HK, Virmani R. Pathology of drug-eluting stents in humans: Delayed healing and late thrombotic risk. *J Am Coll Cardiol* 2006;48:193–202.
59. Resnick N, Yahav H, Shay-Salit A, et al. Fluid shear stress and the vascular endothelium: For better and for worse. *Prog Biophys Mol Biol* 2003;81:177–199.
60. Vey E, Roger C, Meehan L, Booth J, Claybourn M, Miller A, Saiani A. Degradation mechanism of poly(lactic-co-glycolic) acid block copolymer cast films in phosphate buffer solution. *Polym Degrad Stab* 2008;93:1869–1876.
61. Shenderova A, Burke TG, Schwendeman SP. The acidic microclimate in poly(lactide-co-glycolide) microspheres stabilizes camptothecins. *Pharm Res* 1999;16:241–248.
62. Cai Q, Shi GX, Bei JZ, Wang SG. Enzymatic degradation behavior and mechanism of poly(lactide-co-glycolide) foams by trypsin. *Biomaterials* 2003;24:629–638.
63. Pamula E, Menaszek E. *In vitro* and *in vivo* degradation of poly(l-lactide-co-glycolide) films and scaffolds. *J Mater Sci Mater Med* 2008;19:2063–2070.